



## CASE REPORT

# Immunological features of a lung cancer patient achieving an objective response with anti-programmed death-1 blockade therapy

Toshiko Kamata<sup>1,2</sup> | Shigetoshi Yoshida<sup>1</sup>  | Mariko Takami<sup>2</sup> | Fumie Ihara<sup>2</sup> | Hiroko Yoshizawa<sup>2</sup> | Takahide Toyoda<sup>2,3</sup> | Yuichiro Takeshita<sup>4</sup> | Seiichi Nobuyama<sup>4</sup> | Yukiko Kanetsuna<sup>5</sup> | Tetsuo Sato<sup>4</sup> | Ichiro Yoshino<sup>3</sup> | Shinichiro Motohashi<sup>2</sup> 

<sup>1</sup>Department of Thoracic Surgery, School of Medicine, International University of Health and Welfare, Atami Hospital, Atami, Japan

<sup>2</sup>Department of Medical Immunology, Graduate School of Medicine, Chiba University, Chiba, Japan

<sup>3</sup>Department of General Thoracic Surgery, Graduate School of Medicine, Chiba University, Chiba, Japan

<sup>4</sup>Department of Respiriology, Atami Hospital, International University of Health and Welfare, Atami, Japan

<sup>5</sup>Department of Clinical Pathology, Atami Hospital, International University of Health and Welfare, Atami, Japan

## Correspondence

Shigetoshi Yoshida, Department of Thoracic Surgery, School of Medicine, International University of Health and Welfare, Atami Hospital, Atami, Japan.  
Email: shigeyoshida@iuhw.ac.jp

## Funding information

International University of Health and Welfare, School of Medicine; Ministry of Education, Culture, Sports, Science and Technology, Grant/Award Number: 18H02892

## Abstract

The role of immune checkpoint inhibitors in metastatic lung cancer has been established in recent years and the pretherapeutic profiles of the tumor microenvironment in responders have been increasingly reported. The role of salvage surgery and the immune profiles of the posttherapeutic specimens in patients achieving an objective response have rarely been studied. We report a case of metastatic lung cancer treated by anti-programmed death-1 Ab followed by surgical resection. The immune status of the tumor was assessed, showing germinal center formation, memory B cell infiltration, and a high frequency of interferon gamma -secreting T cells.

## KEYWORDS

anti-PD-1 antibody, immunotherapy, lung cancer, surgery, tumor-infiltrating lymphocyte

## 1 | INTRODUCTION

Immune checkpoint inhibitors (ICI) such as anti-programmed death (PD)-1 Abs have a positive impact on antitumor immunity, achieving positive responses in up to 18% of advanced non-small-cell lung

cancer patients.<sup>1</sup> Clinical trials on the feasibility of ICI in a neoadjuvant setting are ongoing and the role of surgery in this setting has yet to be established. Although studies focusing on immunological features that predict positive responses to ICI are frequently reported, there are few studies that focus on the tumor microenvironment following treatment in non-small-cell lung cancer. We report

This is an open access article under the terms of the Creative Commons Attribution-NonCommercial-NoDerivs License, which permits use and distribution in any medium, provided the original work is properly cited, the use is non-commercial and no modifications or adaptations are made.

© 2019 The Authors. *Cancer Science* published by John Wiley & Sons Australia, Ltd on behalf of Japanese Cancer Association.

the results of analysis of the tumor-infiltrating lymphocytes acquired from a patient who underwent surgery for residual disease, following anti-PD-1 Ab therapy.

## 2 | CASE SUMMARY

A 78 year-old-man was diagnosed with squamous cell lung cancer with metastasis to the adrenal gland (c-T2aN0M1b stage IVA). He received 4 courses of chemotherapy (carboplatin and gemcitabine), followed by ICI with nivolumab. Although residual disease in the right upper lobe was detected by chest computed tomography, fluorodeoxyglucose-PET revealed low uptake in both the lung lesion and adrenal gland. After a total of 25 courses of nivolumab were given, surgery was carried out to ascertain the pathological response to the therapy and resect residual disease. The patient is being followed up as an outpatient and shows no evidence of disease recurrence 10 months after surgery.

## 3 | MATERIALS AND METHODS

### 3.1 | Antibodies and reagents

The following Abs, matching isotype controls, and reagents were used in the flow cytometric assays and analyzed with FACSCanto II (BD Biosciences). Phycoerythrin (PE) anti-CD3, peridinin chlorophyll protein complex anti-CD45, allophycocyanin (APC) anti-interleukin (IL)-10, CD86, CD3, Pacific blue (PB) anti-CD4, CD3, FITC anti-CD45RA, CD19, CD56, PE-Cy7 anti-CD20, CD8, and AmCyan anti-CD45 were from BD Biosciences. Allophycocyanin anti-CD38, APC/cyanine 7 (Cy7) anti-CD4, CD19, CD40, PB anti-CD19, Brilliant Violet 510 anti-CD27, PE anti-interferon gamma (IFN $\gamma$ ), IgD, and CD80 were from BioLegend. Anti-Foxp3 (eFluor 660 conjugate) and PE-Cy7 anti-CD83, fixable viability dye (APC-Cy7), and the Foxp3/transcription factor staining buffer set were obtained from eBioscience, and FcR blocking reagent was from Miltenyi Biotec.

### 3.2 | Collection of samples

Peripheral blood was collected before surgery. Fresh tumor samples and normal lung tissue from a different segment were obtained from the surgically resected right upper lobe and stored in MACS tissue storage solution (Miltenyi Biotec) at 4°C until further use. Subcarinal lymph node samples were also obtained and stored.

All experiments were undertaken in accordance with the Declaration of Helsinki and approved by the institutional review board of the International University of Health and Welfare, Atami Hospital (No. 18-A-115) and the Graduate School of Medicine, Chiba University (No. 273). Informed consent was obtained from the patient participating in this study.

The datasets used during the current study are available from the corresponding author on reasonable request.

### 3.3 | Extraction of mononuclear cells

Peripheral blood mononuclear cells were obtained by density gradient separation with Ficoll-Paque PLUS (GE Healthcare Biosciences). Lymph node samples were dissected and resuspended, followed by density gradient separation. Tumor samples were cut into small fragments and dissociated into single cells with a gentle MACS Octo Dissociator with Heaters and the tumor dissociation kit (Miltenyi Biotec), according to the manufacturer's protocol. Mononuclear cells were collected by density gradient separation with 100% and 75% lymphocyte separation medium (MP Biomedicals).

### 3.4 | Cytokine secretion analysis

Interleukin-10 secretion analysis was carried out as follows. Briefly,  $1 \times 10^6$  cells were incubated in 500  $\mu$ L RPMI-1640 complete medium, with 10  $\mu$ g/mL Lipopolysaccharide (L-4391; Sigma Aldrich), 50 ng/mL phorbol 12-myristate 13-acetate (PMA), 1  $\mu$ g/mL ionomycin (Sigma Aldrich), and monensin  $\times 1$  (eBioscience) for 5 hours.

An IFN $\gamma$  secretion assay was carried out, where  $5 \times 10^5$  cells in 200  $\mu$ L RPMI-1640 complete were incubated for 4 hours with 50 ng/mL PMA, 1  $\mu$ mol/L ionomycin, and monensin  $\times 1$ .

Intracellular staining was carried out with BD Cytofix/Cytoperm Fixation Permeabilization kit (BD Pharmingen).

### 3.5 | B cell stimulation assay

Lymphocytes were stained with anti-CD19 FITC and purified using an Auto MACS with anti-FITC beads (Miltenyi Biotec). Cells were incubated at  $3.5 \times 10^4$  cells in 140  $\mu$ L complete medium with 0.4  $\mu$ mol/L ODN 2006 (InvivoGen). Cells were collected after 24 hours and surface markers were assessed by flow cytometry. Culture supernatants were collected for cytometric bead array (BD Biosciences) for cytokines on day 1 and for Ig concentration on day 7.

### 3.6 | Immunohistochemistry

Resected specimens were fixed in 10% formalin. Anti-CD3 (clone PS1), CD8 (clone C8/144B), CD4 (clone 4B12), and CD20 (L26) Abs were purchased from Nichirei Biosciences. Staining with primary and secondary Abs was undertaken in accordance with the manufacturer's protocol.

## 4 | RESULTS

Histology of the resected tumor showed marked fibrosis with vasculitis and foreign body granuloma. Lymphoid follicles were found in the fibrotic area and the surrounding lung (Figure 1A), with germinal center formation in the resected lymph nodes. There was no

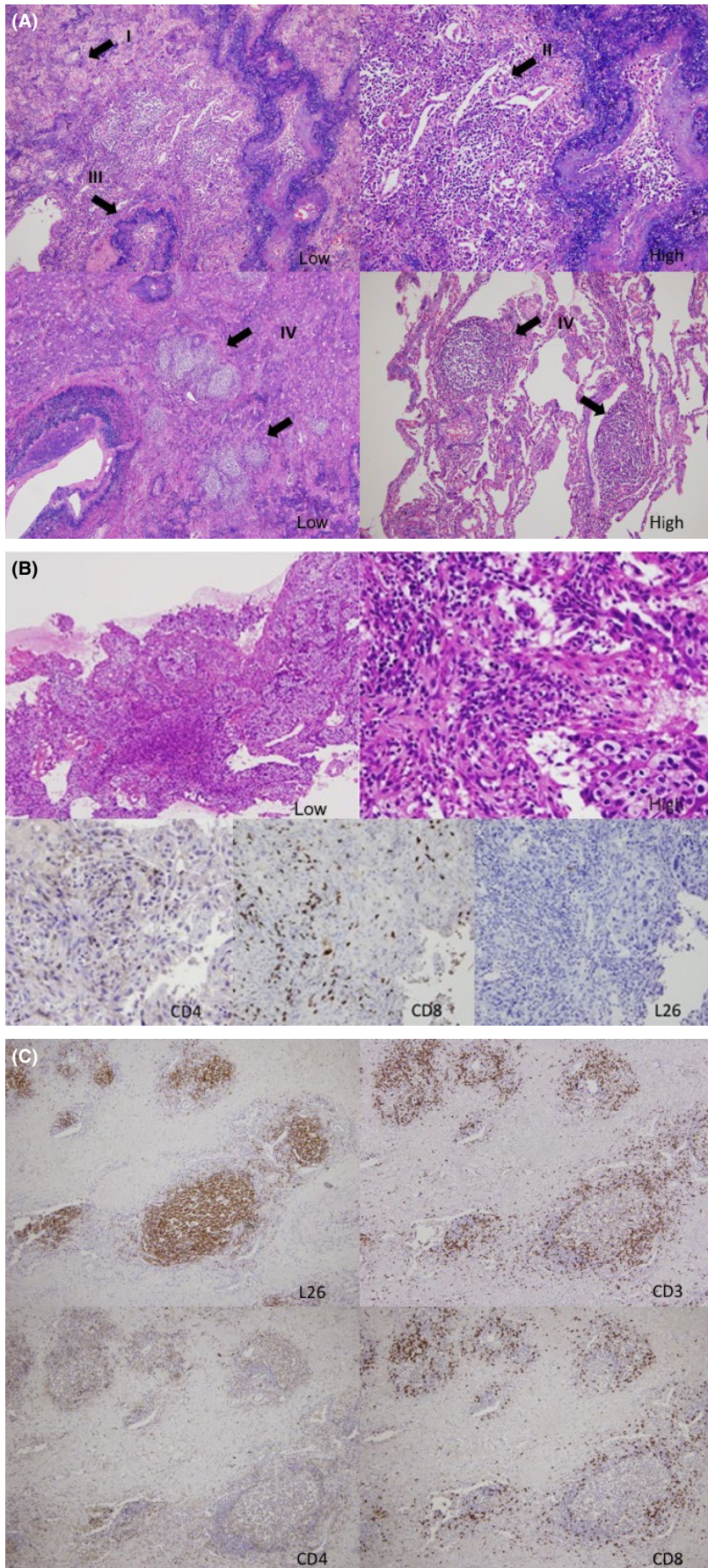


**FIGURE 1** Pathological findings in a lung cancer patient treated with anti-programmed death-1 blockade therapy. A, Victoria blue-H&E staining of the resected lung. The tumor bed showed dense fibrosis (I) with lymphocyte infiltration (II) and vasculitis (III). Germinal centers were found in the tumor bed and normal lung (IV). B, Pathology of the initial transbronchial biopsy specimen. H&E staining (upper panels) revealed sheets of atypical cells with little keratinization. Immunohistochemistry for CD4, CD8, and L26 (lower panels). C, Immunohistochemistry of the resected specimen with L26 (upper left panel), CD3 (upper right panel), CD8 (lower left panel), and CD4 (lower right panel)



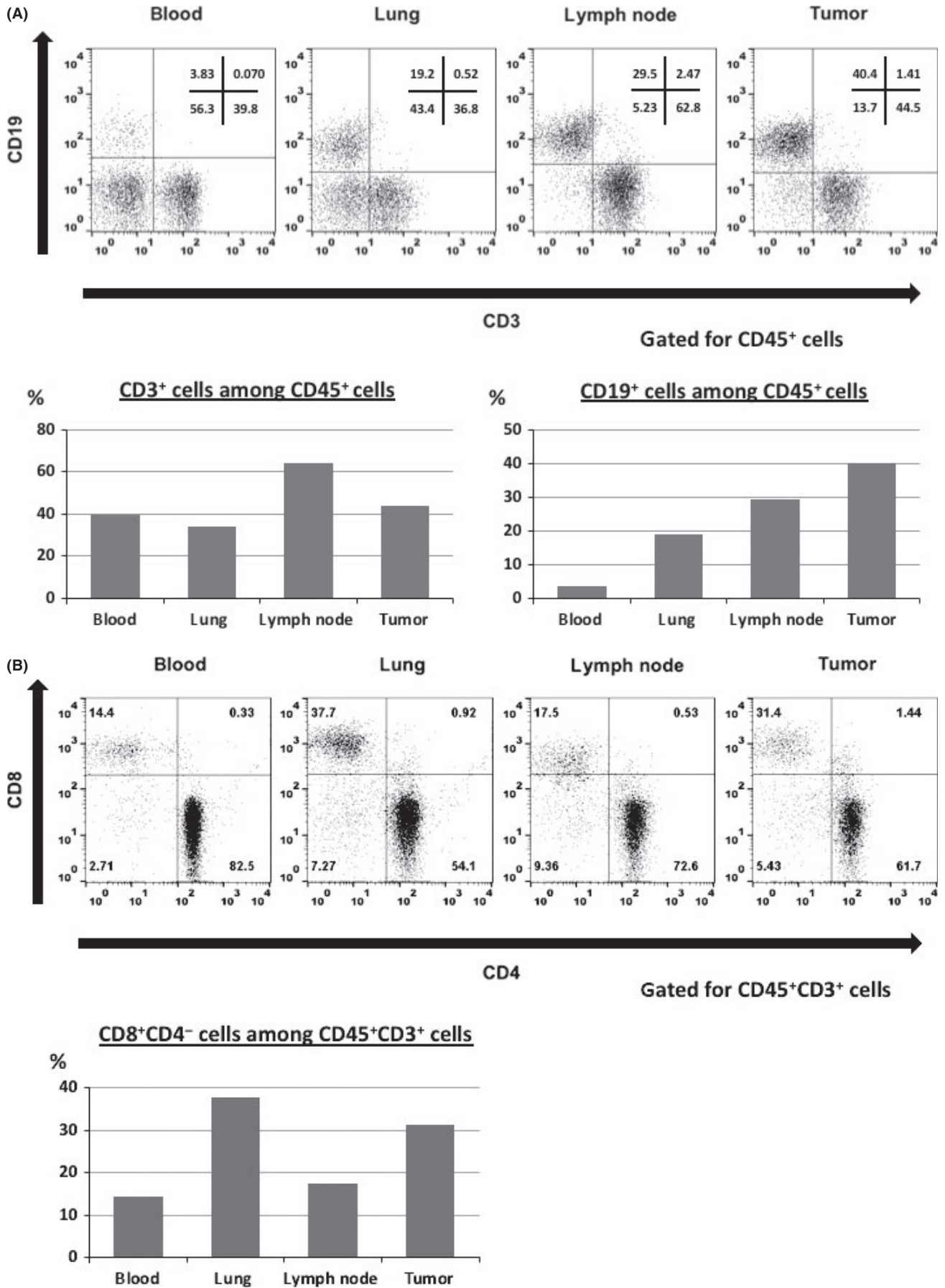
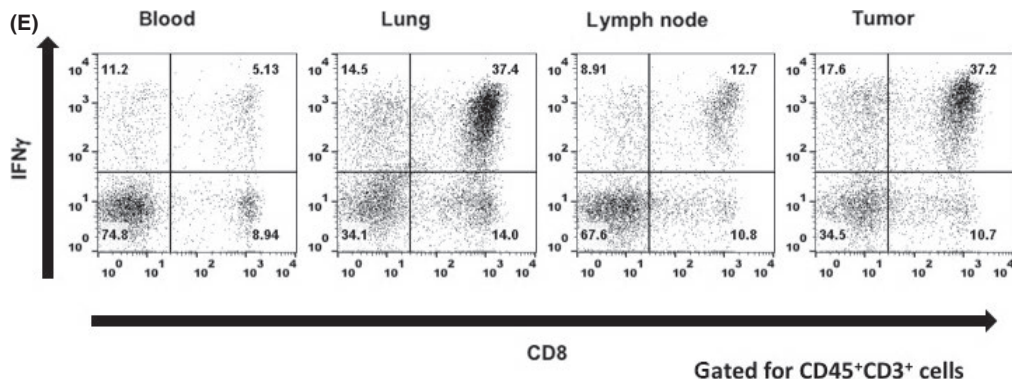
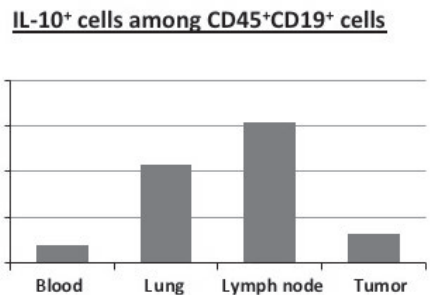
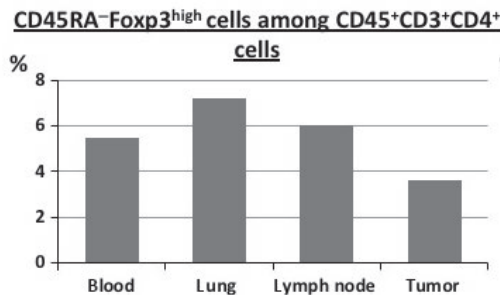
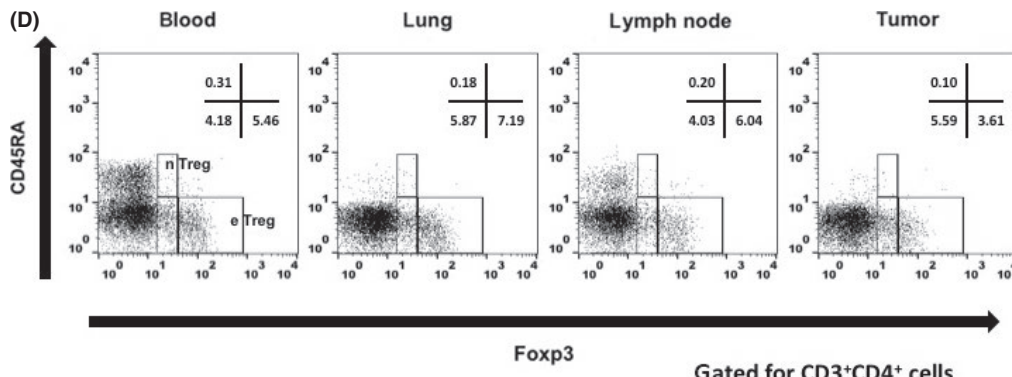
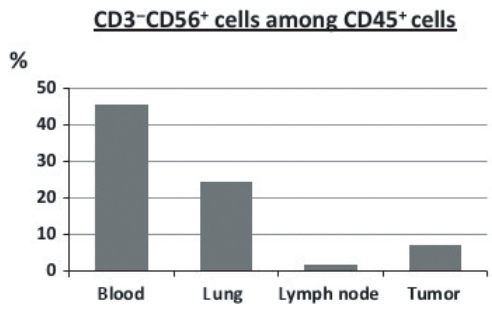
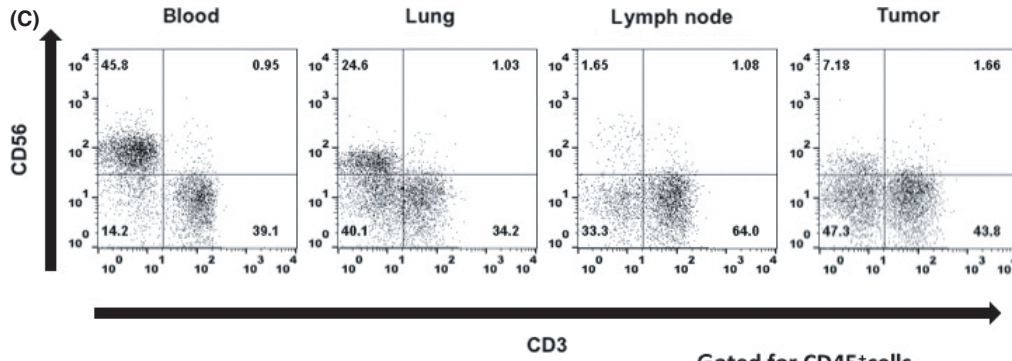


FIGURE 2 (Continued)



**FIGURE 2** Flow cytometric analysis of mononuclear cells in a lung cancer patient treated with anti-programmed death-1 blockade therapy. A-C, Flow cytometric analysis for CD45<sup>+</sup> lymphocytes and percentages of each subset. D, Results of intracellular staining for Foxp3: effector regulatory T (eTreg) cells, CD3<sup>+</sup>CD4<sup>+</sup>CD45RA<sup>-</sup>foxp3<sup>high</sup> cells; naïve regulatory T (nTreg) cells, CD3<sup>+</sup>CD4<sup>+</sup>CD45RA<sup>+</sup>foxp3<sup>low</sup> cells. Percentages of eTreg cells are depicted on the left lower panel. Interleukin (IL)-10-secreting CD19<sup>+</sup> cells following stimulation are depicted on the right lower panel. E, Results of intracellular staining for interferon-gamma (IFN $\gamma$ )

evidence of viable tumor cells. Immunohistochemistry of the initial biopsy specimen showed lymphocyte infiltrates positive for CD4 and CD8. L26 positivity was less than 1% (Figure 1B). CD3<sup>+</sup> cells and L26<sup>+</sup> cells were seen mainly in the lymphoid follicle structures of the resected specimen. CD8<sup>+</sup> cells were predominant among the CD3<sup>+</sup> cells, compared to CD4<sup>+</sup> cells (Figure 1C).

Analysis of the freshly obtained infiltrating lymphocytes revealed that CD19<sup>+</sup> B cells were seen at a high frequency in the tumor bed compared with normal lung tissue, blood, and lymph nodes (Figure 2A). CD8<sup>+</sup> cells among CD3<sup>+</sup> T cells were at a high frequency in the tumor bed and normal lung tissue (Figure 2B). CD3<sup>-</sup>CD56<sup>+</sup> natural killer cells were seen mainly in the normal lung tissue and peripheral blood (Figure 2C).

The CD45RA<sup>-</sup>Foxp3<sup>high</sup> CD4 T cells, classified as effector regulatory T (eTreg) cells and IL-10 secreting regulatory B (Breg) cells were found at a low frequency in the tumor bed (Figure 2D). More than 70% of the CD8 T cells in the tumor bed and normal lung tissue secreted IFN $\gamma$  on stimulation with PMA and ionomycin, which was twice as high as lymphocytes from the peripheral blood (Figure 2E). CD27<sup>+</sup> memory cells were found at a high frequency in the tumor bed and lymph nodes compared with the other sites (Figure 3A). Baseline CD80 and CD83 expression was higher in tumor-derived B cells (Figure 3B). There was no difference in the CD86 expression and upregulation following stimulation between the 4 sites. Conversely, CD40 upregulation following stimulation was enhanced in the lymph node and tumor compared with the peripheral blood (Figure 3C). Interleukin-10 could be detected at a low level in the supernatant from tumor-derived B cells, but tumor necrosis factor (TNF) was also secreted at a higher level compared with the peripheral blood and lymph nodes (Figure 3D). Secretion of IgM was particularly enhanced in the lymph node tissue following stimulation, whereas IgA and IgG were found at lower or comparable levels to other sites (Figure 3E).

## 5 | DISCUSSION

There are few reports on surgical resection in lung cancers following ICI. Chaft et al reported 5 patients with metastatic cancer, who underwent resection following ICI therapy. Surgery was carried out successfully and 2 patients had a complete response despite residual disease evident on chest computed tomography. Four patients remained disease-free 7-23 months postoperatively.<sup>2</sup> Forde et al undertook a phase II clinical trial including patients with resectable lung cancer, receiving anti-PD-1 blockade therapy in a neoadjuvant setting, with 45% of patients achieving a major pathological

response.<sup>3</sup> A further report on the histological features described the regression bed, which referred to the peripheral replacement of tumors with a fibroinflammatory area.<sup>4</sup> Patients with major pathological responses had dense immune infiltrates, characterized by tertiary lymphoid structures accompanied by proliferative fibrosis and neovascularization.

According to a recent review, tumor-infiltrating B cells localize to form and maintain tertiary lymphoid organs within the tumor. B cells react to tumor antigens and differentiate into plasma cells to produce tumor-specific Abs. Furthermore, B cells promote T cell-mediated immune responses through antigen presentation.<sup>5</sup> High density of follicular B cells is reportedly associated with improved survival and a higher proportion of reactivity to tumor-associated antigens in the tumor microenvironment.<sup>6</sup> Conversely, Breg cells that produce IL-10 and transforming growth factor- $\beta$  have been reported to promote Treg cells and inhibit antitumor immunity.<sup>7</sup> In a study on chronic virus infection in Macaques, PD-1 was highly expressed on memory B cells. Blockade of PD-1 resulted in increased proliferating memory B cells and Ab titers.<sup>8</sup> An in vitro study on human B cells showed decreased proliferation and Ig secretion with PD-1-PD-ligand 1 interactions.<sup>9</sup>

Upregulation of CD40 expression on B cells following stimulation is reported to be diminished in advanced cancer patients with a decreased percentage of CD27<sup>+</sup> cells.<sup>10</sup> Although CD27<sup>+</sup> memory cells are reportedly found at a higher percentage in the tumor, CD19<sup>+</sup> cells are reported to be at a comparable level with the peripheral blood.<sup>11</sup> The accumulation of B cells and the abundant germinal center formation found in the posttreatment specimen of the patient presented here is a characteristic feature in accordance with the report by Cottrell et al.<sup>4</sup> The increase in CD19<sup>+</sup> cells and CD27<sup>+</sup> cells and upregulation of costimulatory molecules found in the tumor and lymph nodes of our patient could be the result of anti-PD-1 blockade. This might have led to improved antigen presentation and costimulation from the B cells. Furthermore, analysis of B cells revealed an increased capacity to secrete TNF in the tumor, which is reported to induce T helper-1 (Th1) responses.<sup>12</sup> These B cell features might have subsequently caused the high Th1 response and tumor regression. The B cells derived from the lymph node also secreted high levels of IgM with Toll-like receptor-9 stimulation (Figure 3E), in spite of the fact that the fraction of non-class-switched memory B cells was at a comparable level to other sites (Figure 3A). From this finding we deduce that IgM memory B cells with a high capacity to secrete immunoglobulins against tumor antigens accumulated into the regional lymph nodes, which could be due, in part, to PD-1 blockade.

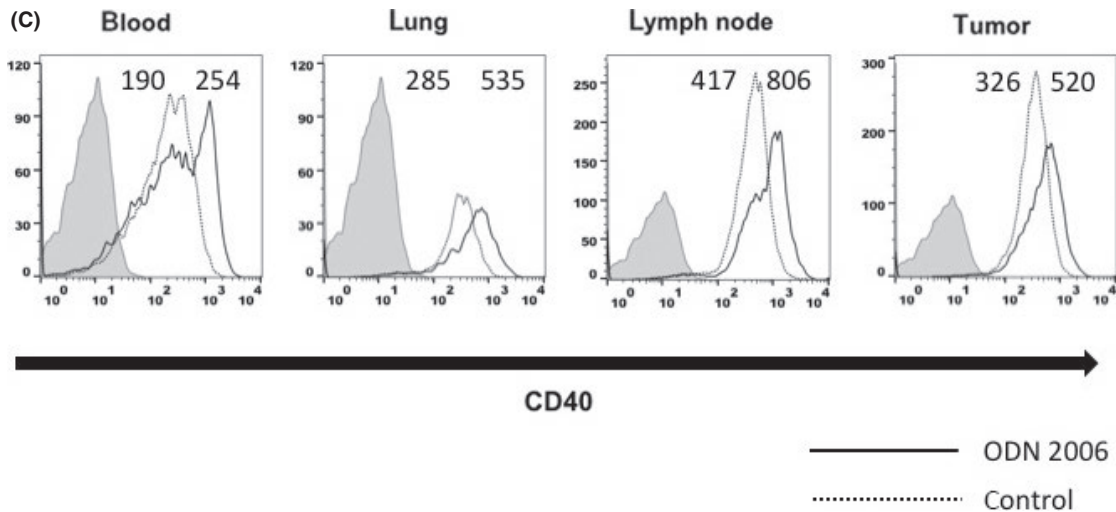
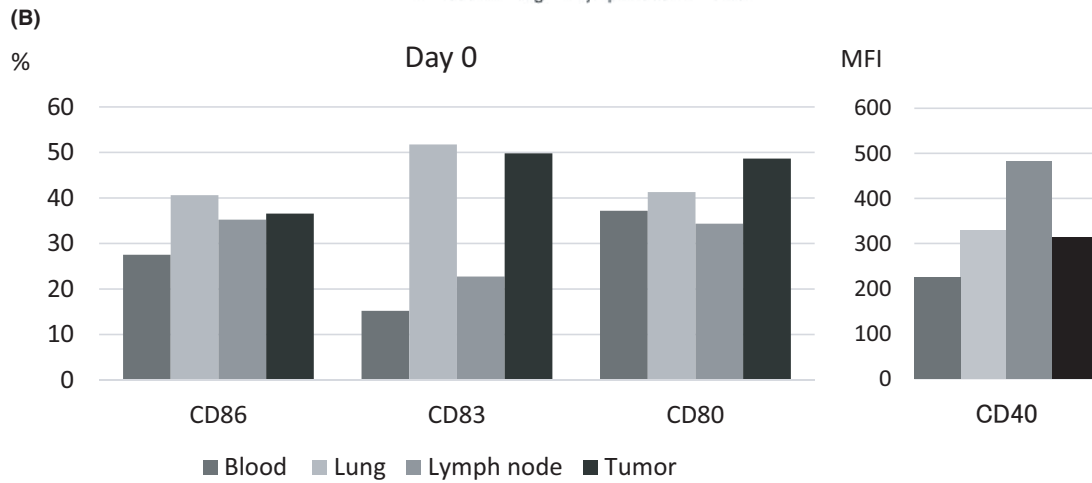
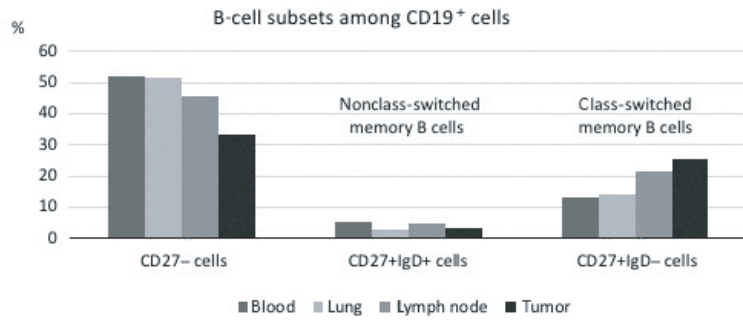
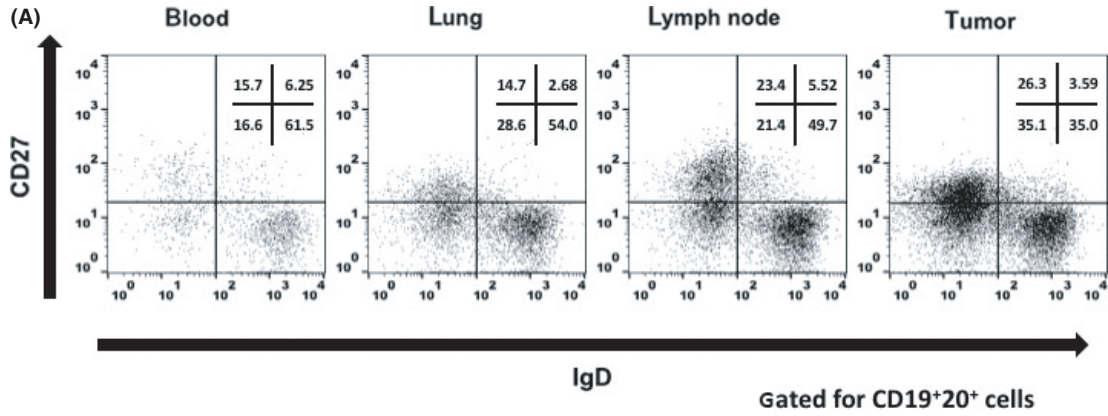
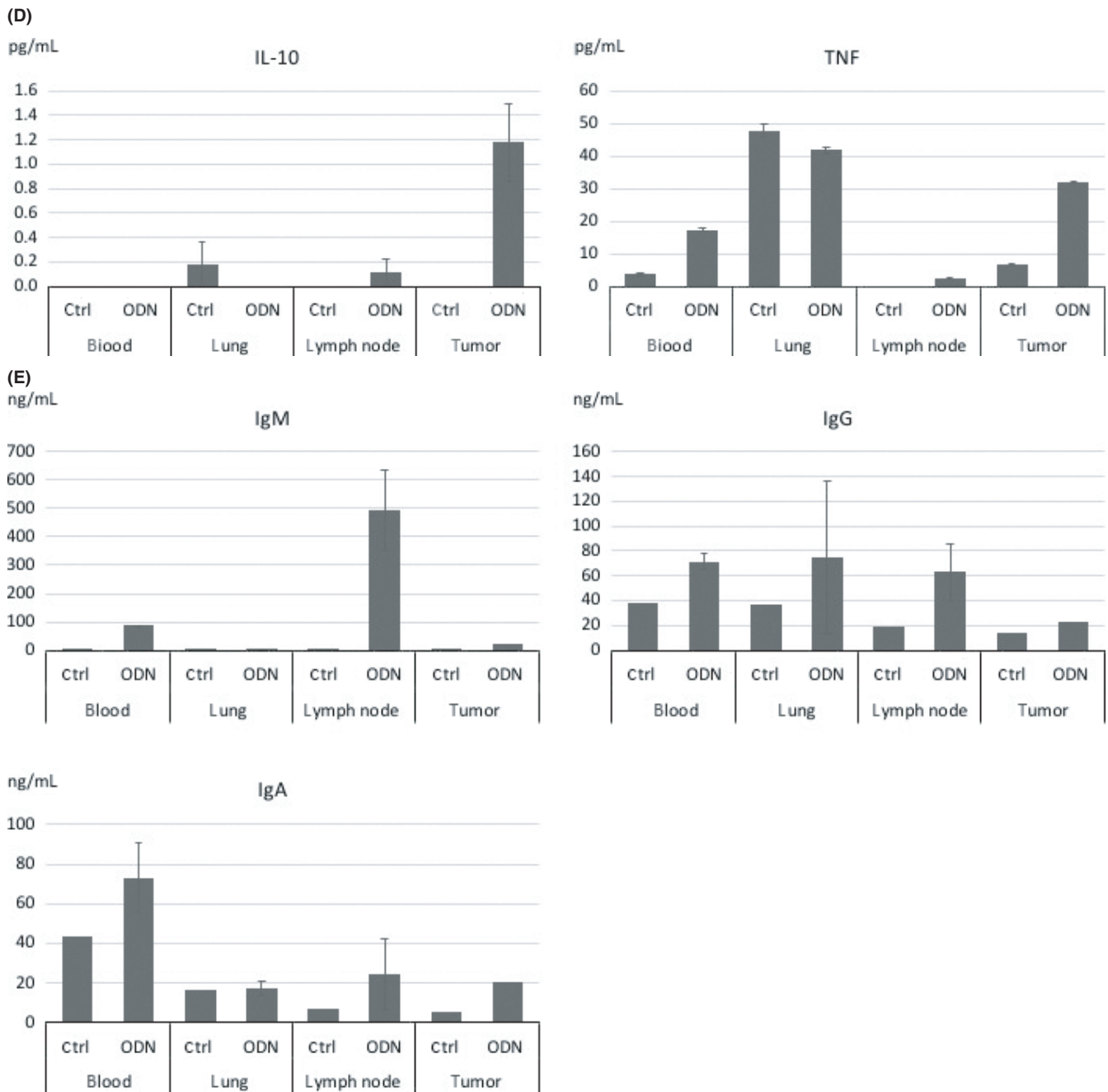


FIGURE 3 (Continued)





**FIGURE 3** Flow cytometric analysis and functional assays on B cells. A, Flow cytometric data on CD19<sup>+</sup>CD20<sup>+</sup> cells and percentage of B-cell subsets. B, Positivity of CD86, CD83, CD80 (population comparison method), and CD40 (median fluorescence intensity; MFI). Purified CD19<sup>+</sup> cells were simulated with oligodeoxynucleotide (ODN) 2006. C, Surface staining of stimulated (ODN) or nonstimulated cells (Ctrl) after 24 h. The shaded histogram is the isotype control. The MFI of CD40 is depicted. D, Results of cytometric bead arrays (CBA) on cell culture supernatants, carried out in duplicate. E, CBA analysis for immunoglobulins were undertaken on day 7. The average and SD of 2 different wells are depicted. TNF, tumor necrosis factor

Our analysis was undertaken on a single patient with no flow cytometric data from the pretreatment specimen. Further analysis of samples before and after therapy are needed to reach any major conclusion. However, surgical resection and immunological assays carried out following PD-1 blockade are rare, and this research could provide further insight into the response mechanism and histological features of the treatment.

#### ACKNOWLEDGMENTS

We thank Toshinori Kiriara, Yoshimi Endo, and Shota Okahara for their excellent technical assistance. This research was supported by grants from the International University of Health and Welfare, School of Medicine and the Ministry of Education, Culture, Sports, Science and Technology (Japan; Grants-in-Aid: Scientific Research,



(B) #18H02892). We thank S. J. Win, PhD, from Edanz Group for editing a draft of this manuscript.

## DISCLOSURE

The authors disclose no potential conflicts of interest.

## ORCID

Shigetoshi Yoshida  <https://orcid.org/0000-0001-5571-886X>

Shinichiro Motohashi  <https://orcid.org/0000-0002-9332-3129>

## REFERENCES

1. Topalian SL, Hodi FS, Brahmer JR, et al. Safety, activity, and immune correlates of anti-PD-1 antibody in cancer. *N Engl J Med*. 2012;366:2443-2454.
2. Chaft JE, Hellmann MD, Velez MJ, Travis WD, Rusch VW. Initial experience with lung cancer resection following treatment with T cell checkpoint inhibitor therapy. *Ann Thorac Surg*. 2017;104:e217-e218.
3. Forde PM, Chaft JE, Smith KN, et al. Neoadjuvant PD-1 blockade in resectable lung cancer. *N Engl J Med*. 2018;378:1976-1986.
4. Cottrell TR, Thompson ED, Forde PM, et al. Pathologic features of response to neoadjuvant anti-PD-1 in resected non-small-cell lung carcinoma: a proposal for quantitative immune-related pathologic response criteria (irPRC). *Ann Oncol*. 2018;29:1853-1860.
5. Wang SS, Liu W, Ly D, Xu H, Qu L, Zhang L. Tumor-infiltrating B cells: their role and application in anti-tumor immunity in lung cancer. *Cell Mol Immunol*. 2019;16:6-18.
6. Germain C, Gnjjatic S, Tamzalit F, et al. Presence of B cells in tertiary lymphoid structures is associated with a protective immunity in patients with lung cancer. *Am J Respir Crit Care Med*. 2014;189:832-844.
7. Rosser EC, Mauri C. Regulatory B cells: origin, phenotype, and function. *Immunity*. 2015;42:607-612.
8. Velu V, Titanji K, Zhu B, et al. Enhancing SIV-specific immunity in vivo by PD-1 blockade. *Nature*. 2009;458:206-210.
9. Buermann A, Römermann D, Baars W, Hundrieser J, Klempnauer J, Schwitzer R. Inhibition of B-cell activation and antibody production by triggering inhibitory signals via the PD-1/PD-ligand pathway. *Xenotransplantation*. 2016;23:347-356.
10. Carpenter EL, Mick R, Rech AJ, et al. Collapse of the CD27+ B-cell compartment associated with systemic plasmacytosis in patients with advanced melanoma and other cancers. *Clin Cancer Res*. 2009;15:4277-4287.
11. Zirakzadeh AA, Marits P, Sherif A, Winqvist O. Multiplex B cell characterization in blood, lymph nodes, and tumors from patients with malignancies. *J Immunol*. 2013;190:5847-5855.
12. Romero-Ramírez S, Navarro-Hernandez I, Cervantes-Díaz R, et al. Innate-like B cell subsets during immune responses: beyond antibody production. *J Leukoc Biol*. 2018;105(5):843-856.

**How to cite this article:** Kamata T, Yoshida S, Takami M, et al. Immunological features of a lung cancer patient achieving an objective response with anti-programmed death-1 blockade therapy. *Cancer Sci*. 2020;111:288-296. <https://doi.org/10.1111/cas.14222>